THE JOURNAL OF PHYSICAL CHEMISTRY B

Article

pubs.acs.org/JPCB

How Does Glycerol Enhance the Bioprotective Properties of Trehalose? Insight from Protein−Solvent Dynamics

Giuseppe Bellavia,* Laurent Paccou, Yannick Guinet, and Alain Hédoux

UMET, UFR de Physique, BAT P5 UMR CNRS 8207, Université Lille 1, 59655 Villeneuve d'Ascq, France

ABSTRACT: We present Raman investigations on lysozyme/trehalose/glycerol solutions at low water content, from room temperature up to the occurrence of the protein thermal denaturation. We studied the Amide I band and the low-frequency spectrum as a function of the glycerol content. The former allows us to monitor the protein unfolding; the latter probes the protein and solvent dynamics in anharmonic and quasi-harmonic regimes. It was shown that adding a small amount of glycerol to trehalose stiffens the dry matrix in which proteins are embedded, thus improving their stability. The analysis of the Amide I band reveals that glycerol enhances the stabilization effect of trehalose on proteins for low water content, but still liquid, systems. Data show that the protein unfolding temperature has a maximum value around 5% Glyc/TRE g/g. The overlapping low-frequency contributions, corresponding to fast anharmonic and quasi-harmonic motions, respectively, related to the mean square displacement $\langle u^2 \rangle$ and the vibrational density of states (VDOS) usually determined by neutron scattering experiments, have been carefully analyzed to understand the effect of glycerol. The intensity of the quasi-elastic scattering (QES) peak reveals a dynamical-like transition at high temperatures, close to the denaturation temperature. This one, as well as the low-frequency vibrational modes, reflects the same enhanced trend of the Amide I band with respect to the glycerol concentration, but at lower temperatures. A linear correlation is found among the transition temperatures of both the dynamical-like transition and the low-frequency modes, as well as the temperature dependent change of the Amide I frequency. This confirms the solvent dynamics as a necessary precursor to promote protein unfolding. Glycerol antiplasticizes the matrix with respect to the trehalose by enhancing the stability of the protein in a more rigid trehalose/water/glycerol matrix. As expected from the analysis of the Amide I band, the maximum effect of glycerol on trehalose is determined for 5% Glyc/TRE content.

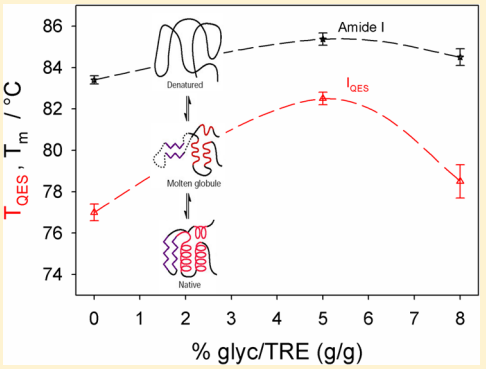

INTRODUCTION

Proteins are essential components for living beings. Their functionality is strictly related to their stability. This is of great interest concerning both basic science and biotechnological applications in food, drug, and tissue storage. High levels of disaccharides, in particular, trehalose,[1] were found in organisms which adopt a dormant state when adverse environmental conditions are fulfilled.[2,3] As long as the mechanism behind biopreservation is still a matter of debate, many hypotheses have been formulated. Some models face the problem from a thermodynamics point of view and they take into account the interfacial water and the protein nearest-neighbor. In this context, the mechanism to retain the native protein conformation is supposed to be related to the suppression of conformational fluctuations by preferentially excluding, otherwise trapping, water from the first hydration shell.[4−6] A further way to understand the issue is from a dynamical point of view, in which the protein degradation is slowed down because of the coupling between the cosolvent and the hosted protein[7−14] or by the cosolvent viscosity which causes the inhibition of the large-amplitude vibrations and the hindrance of the dynamics of the protein.[15] The latter is based mainly on the properties of the cosolvent, i.e., the trehalose, with no regard to the protein. The former three models are likely biomolecule-dependent, because the biopreservation effect is strictly related to the presence of the biomolecule, i.e., the stability mechanism looks to appear exclusively in the presence of the protein.[8] Thus, by studying only biopreserving systems with no biomolecules embedded in them, full comprehension of the bioprotection mechanism could not be acquired. Nevertheless, properties of a binary water−sugar system, the glass transition, for instance, do not have a simple correlation with the bioprotection efficacy of the bioprotectant; any significant interaction terms should be triggered only by the presence of the protein.

Recent studies showed that the stability of proteins is considerably improved by adding a small amount of glycerol to trehalose.[16−19] It was evidenced by the way, by redissolving several enzymes previously freeze-dried in different trehalose−glycerol mixtures, the deactivation time of each investigated enzyme was dependent on the glycerol content with a maximum at about 5% glyc/TRE in weight.[16] Dry glycerol−trehalose glassy systems with no protein were then analyzed by incoherent neutron scattering. Despite T_g depending monotonically on the glycerol content, the $\langle u^2 \rangle$ from the Debye−

Received: January 20, 2014
Revised: July 2, 2014

   dx.doi.org/10.1021/jp500673b | J. Phys. Chem. B XXXX, XXX, XXX−XXX

Waller formalism provides the stiffest glassy environment again for 5% glyc/TRE.[17] Afterward it was found that the binary system shows a minimum in the efficiency whereby relaxation occurs[17] at the same glycerol content found earlier. Further quasi-elastic neutron scattering and also inelastic neutron scattering measurements on binary glyc/TRE mixtures were performed,[20,21] confirming the previous findings. The suppression of the fast dynamics of trehalose by glycerol was associated with the change of the hydrogen-bond (H-bond) network of the system as it appears in the average lifetime and the occupancy of the H-bonds.[17,20−25] This behavior could be explained by the hole-filling model[26,27] which points out how glycerol can play the role of antiplasticizer (decreasing T_g) with respect to trehalose. This would fill the empty space among trehalose and protein, and possibly would change the stiffness of the H-bond network, thus hindering the protein residual fluctuations and giving stability. However, this model, based solely on geometrical meshing, does not manage to fully explain the fact. For instance, the protein−solvent electrostatic interaction energies are a worthy contribution to stabilize the system,[25] with no regard to the protein size.[12]

Fast conformational fluctuations of the protein might be the key precursors to the larger structural and global protein motions.[28] Moreover, a relation between fast and slow relaxation processes was also found,[18] which implies a reduction in the amplitude of local molecular motions together with an improved protein stability.[29] In this respect, it was shown that the simultaneous analysis of the Amide I region and the low-frequency Raman spectrum (LFRS) brings out crucial information on the denaturation mechanism of proteins in aqueous solution.[30−36] The Amide I band probes the secondary structure of the protein while investigations on the LFRS provide information on protein and solvent dynamics and their coupling. The LFRS is mainly composed of two components, the quasi-elastic scattering one and the low-frequency vibrational one. The former probes the β-fast relaxations, corresponding to anharmonic motions and strongly temperature dependent, which drive cooperative phase transitions, such as the glass transition.[37] The latter gives information on the transformations of the hydrogen-bond (H-bond) network of the solvent.[33] These investigations have shown that structural transformations in the H-bond network of bulk water induced changes in the protein dynamics. In particular, it has revealed that the main bioprotective effect of disaccharides was the strengthening of the H-bond network of water, inducing the reduction of the contribution of anharmonic motions, and the stabilization of the protein at the high temperatures. In this context, new information, related to the influence of the addition of a small amount of glycerol in trehalose/water/protein solutions, can be expected by conducting Raman experiments simultaneously in the low-frequency and Amide I regions on these solutions upon heating. Lysozyme (LSZ) was chosen as model protein since it gives a very low fluorescence contribution to the Raman spectrum.

MATERIALS AND METHODS

Sample Preparations. Lyophilized chicken egg white lysozyme (14.7 kDa) was purchased from Sigma (Sigma, St. Louis, MO) and used without further purification. High-purity dihydrate trehalose (α-D-glucopyranosyl-α-D-glucopyranoside, $C_{12}H_{22}O_{11}$, 342.3 Da) and glycerol anhydrous (1,2,3-propanetiol, $C_3O_3H_8$, 92.1 Da) were supplied from Fluka. Bi-distilled water was used.

Samples were prepared by freeze−drying together lysozyme, trehalose, and glycerol from water solutions by keeping the trehalose/protein concentration ratio constant (1/1 g/g, corresponding to ∼40 TRE/LSZ mole ratio), while the chosen glycerol/trehalose weight ratios were 0%, 5%, and 8% content (corresponding to ∞, 5.4, 3.4 TRE/glyc mole ratio). According to previous studies,[12] a constant TRE/LSZ mole ratio of 40 approaches concentrations within *in vivo* anhydrobiotic systems, along with avoiding the occurrence of crystallization. The samples were then redissolved in water at ∼50% TRE/water by weight, corresponding to ∼40 water/trehalose mole ratio (∼160 water/LSZ mole ratio). This low water concentration is very close to the threshold concentration for a homogeneous sample before phase separation occurs.[13] The system is then a highly viscous liquid. In the following the samples will be indicated as LWT50G#, # indicating, respectively, 0%, 5%, 8% glyc/TRE g/g.

Raman Measurements. Raman spectra were collected for several temperatures, ranging suitably from 20 to 100 °C. For the 1500−1750 cm^{-1} frequency range (Amide I band) a Renishaw spectrometer was used with a Coherent 514.5 nm Ar laser and 20 mW of incident power. The laser spot has a 2 μm diameter and a 20 μm depth, using X50 long-working-distance objective. Solutions were putted into a Linkam quartz cell top filled and sealed to avoid evaporation of water; the temperature control was performed by a Linkam FDCS196 system. The temperature steps changed according to a heating rate of 5 K min^{-1}. By monitoring the spectrum this was estimated to be slow enough to avoid remarkable thermal fluctuations as well as eventual degradation of the sample. It also granted a fast stabilization of the temperature (<2 min) before the spectral acquisition. Each spectrum was then collected 20 times for 10 s at each fixed temperature.

The low-frequency Raman spectra were recorded in the 10−620 cm^{-1} by measuring in backscattering geometry and using a XY Dilor spectrometer. Here, solutions were put into sealed spherical Pyrex cells of about 5 mm diameter, then irradiated with the 514.5 nm line of a mixed Ar−Kr laser and 20 mW of incident power. The spectra were recorded following the same temperature protocol described above for the Renishaw.

Raman Analysis. Figure 1 shows a representative thermal evolution of the Amide I band. The spectra were normalized in the whole referred range, after a subtraction of a suitable linear baseline, and then fitted with 4 Gaussian curves by Peakfit, as illustrated in the inset of Figure 1. For this purpose, a least-squares minimization of the Levenberg−Marquardt nonlinear fitting was performed. For each peak position obtained by the fitting procedure, the corresponding standard deviation error is referred as the error bar.

The spectrum in this region is only composed of Raman bands related to the protein conformation,[38] without any contribution of trehalose and glycerol vibrations.[33,35] The Amide I band is mainly attributed to the C═O stretching vibration of amide groups coupled to the in-phase bending of the N—H bond and the stretching of the C—N bond.[39] The frequency of its intensity maximum (∼1650 cm^{-1}) reflects the nature of the secondary structure of lysozyme, mainly composed of helices. The Amide I frequency is highly dependent on intramolecular C═O···H H-bonds within helices, existing in the folded state and not in the unfolded

dx.doi.org/10.1021/jp500673b | J. Phys. Chem. B XXXX, XXX, XXX−XXX

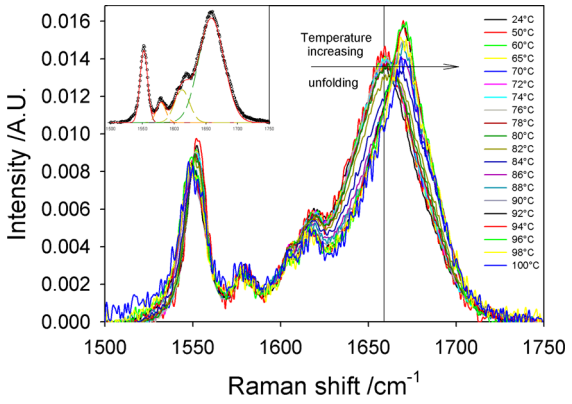

Figure 1. Raman spectra in the 1500−1750 cm^{-1} frequency range for LWT50G0 going from 24 °C up to 100 °C, as indicated by the arrow. The 1659 cm^{-1} position of the peak corresponding to the Amide I band is marked. Inset: representative Raman spectrum of LWT50G0 (symbols) and the fit (red line) together with the spectral decomposition (dashed lines) at 24 °C.

state. Therefore, the plot of the temperature dependence of the Amide I peak position provides a thermal denaturation curve.[40]

It is well-known that the low-frequency Raman spectra of disordered molecular systems are characterized by the overlap of the relaxational and vibrational components.[41] The Raman intensity was formerly converted into reduced intensity (I_r) to obtain Raman spectra free of band shape distortion due to thermal population effects, according to

$$I_r = \frac{I_{\mathrm{Raman}}}{[n(\nu) + 1]\nu} \tag{1}$$

where $n(\nu) = (1/(e^{-k_B T/h\nu} - 1))$ is the Bose factor.[33,42] In order to obtain the separated contributions of QES (I_{QES})[36] and vibrational (I_{vibr}) intensities, the reduced spectra were fitted with a 0 cm^{-1} centered Lorentzian-shape curve for I_{QES} and a log-normal curve for I_{vibr}, six Gaussian curves which take into account all the bands present in the investigated region of the spectrum, and a linear baseline which was then removed.

In order to plot $I_{\mathrm{QES}}(T)$, the reduced intensity was first normalized by the integrated intensity in the 70−170 cm^{-1} range. It is worth noting that this frequency range, mainly corresponding to the vibrational contribution, shows a weak temperature dependence, while the feature around 175 cm^{-1}, due to H-bond stretch motions, depends linearly on temperature.[43] I_{QES} was then determined by integrating the reduced intensity in the 10−30 cm^{-1} range to avoid the contribution of the vibrational component. I_{QES} exhibits the same thermal behavior of the relaxational contribution of $\langle u^2 \rangle$ in neutron scattering Debye−Waller formalism,[44] and therefore it is interpreted as representative of the latter one,[36] notwithstanding a different temperature range.

After removing the QES component from the reduced Raman spectrum, the Raman susceptibility is obtained from

$$\chi''(\nu) = \nu \cdot I_r(\nu) = \frac{C(\nu)}{\nu} G(\nu) \tag{2}$$

where $C(\nu)$ is the light-vibration coupling coefficient and $G(\nu)$ is the vibrational density of states (VDOS) usually measured by inelastic neutron scattering.[45] We recall that the I_r spectrum has the same features of $\chi''(\nu)$ but is more stretched. It was found that $\chi''(\nu)$ is a close representation of the VDOS for rigid and small disordered molecules.[46,47] For larger and more flexible molecules, proteins for instance, it is expected that internal vibrations overlap with collective vibrations. $\chi''(\nu)$ of dry LSZ can be considered as corresponding to the quasi-harmonic dynamics of LSZ including low-frequency internal vibrations which corresponds to the distortion motions of some elements of the secondary structure.[32] The Raman susceptibility of LSZ solutions can be interpreted by comparing its spectrum with those of water, trehalose, and dry LSZ. Figure 2 shows a

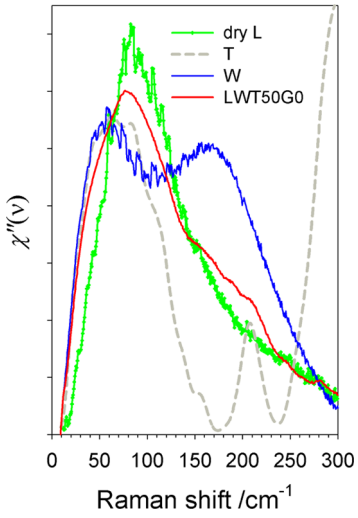

Figure 2. Raman susceptibility spectra at 24 °C for LWT50G0 compared to dry LSZ, water, trehalose, in the 10−300 cm^{-1} frequency range.

comparison of $\chi''(\nu)$ in the 10−300 cm^{-1} frequency range among the LSZ-TRE-water system and each single component at 24 °C. The main part of the spectrum, which peaked around 80 cm^{-1}, usually described by a log-normal curve, can be mainly attributed to complex motions involving the protein dynamics but distinct from H-bond stretch motions found at higher frequencies.[48] Two Gaussian functions are needed to satisfactorily fit the $\nu_{\mathrm{OH\cdots O}}$ band corresponding to the intermolecular OH stretching vibrations in the H-bond network of the solvent: the lower frequency component (G_{W}), centered around 164 cm^{-1}, and the higher frequency one (G_{T}), centered around 202 cm^{-1}. The former will take into account for the tetrahedral structure of the water, as well as the latter is related to the distorted tetrahedral structure and a stiffened H-bond network due to the presence of trehalose.[33,36] To our glycerol concentrations, no additional feature due to glycerol is detectable in the LFRS. A representative thermal evolution of $\chi''(\nu)$ is shown in Figure 3, together with a representative fitting illustrated in the inset.

RESULTS AND DISCUSSION

Amide I Band Analysis. Figure 1 shows a Raman spectra ensemble in the 1500−1750 cm^{-1} frequency range for LWT50G0, as a function of the temperature. Raman spectra for LWT50G5 and LWT50G8 show the same behavior and the same features as well. The protein secondary structure is stabilized by internal C═O···H bonds, inducing the position of the Amide I band. By increasing the temperature the C═O···H bonds break down, making harder C═O stretching vibrations and then inducing the shift toward the higher frequencies of Amide I band.

dx.doi.org/10.1021/jp500673b | J. Phys. Chem. B XXXX, XXX, XXX−XXX

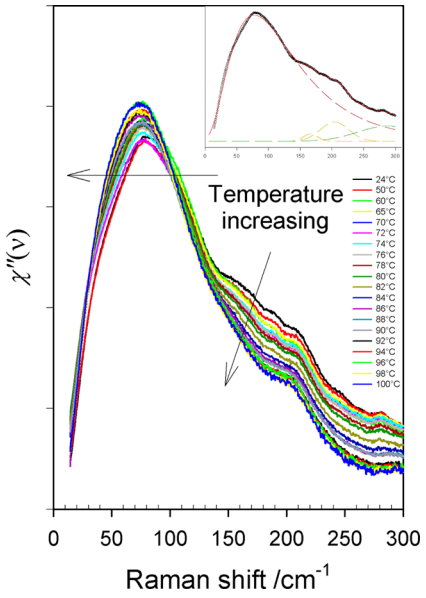

Figure 3. Raman susceptibility spectra in the 10−300 cm^{-1} frequency range for LWT50G0 going from 24 °C up to 100 °C, as indicated by the arrows. Inset: representative Raman susceptibility spectrum of LWT50G0 (symbols) at 24 °C in the 10−300 cm^{-1} frequency range, and the fit (red line) together with the spectral decomposition (dashed lines).

Figure 4 shows the Amide I peak frequency as a function of the temperature for LWT50G# samples at different glycerol

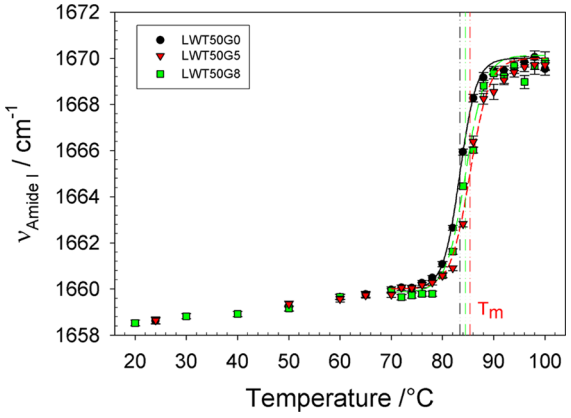

Figure 4. Amide I Raman shift as a function of the temperature for LWT50G#: 0% (black circles), 5% (red triangles), 8% (green squares). Lines are fitting in terms of eq 3. Error bars correspond to ±1 SD from fitting.

content. We can observe that the LWT50G5 data are shifted toward higher temperatures with respect to the other two comparing samples. This means the occurrence of an additional stabilization effect for 5% Glyc/TRE content compared to 0% and 8% on protein thermal denaturation. This is the first time that this feature has been observed in solution. Nonetheless, we have not detected it in more dilute (5 times) solutions (data not shown). Indeed, our solutions are just below the solubility threshold of the system.[12] By following the Raman shift frequency as a function of the temperature T, the midpoint temperature (T_m) of the protein unfolding is estimated via the formula[33]

$$\nu(T) = \frac{\nu_N - \nu_D}{1 + e^{T - T_m/\Delta T}} + \nu_D \quad (3)$$

where ν_N and ν_D represent the frequency values for the native and denaturated states, respectively, and $2{\cdot}\Delta T$ is the temperature domain of the transition. It is noteworthy that the T_m value corresponding to 5% Glyc/TRE is higher than all the other concentrations, drawing a maximum of T_m vs the glycerol content around this value, in agreement with previous results on TRE/glyc mixtures.[17,20]

Low-Frequency Raman Analysis. Figure 5 shows I_{QES} as a function of the temperature for LWT50G#. According to its

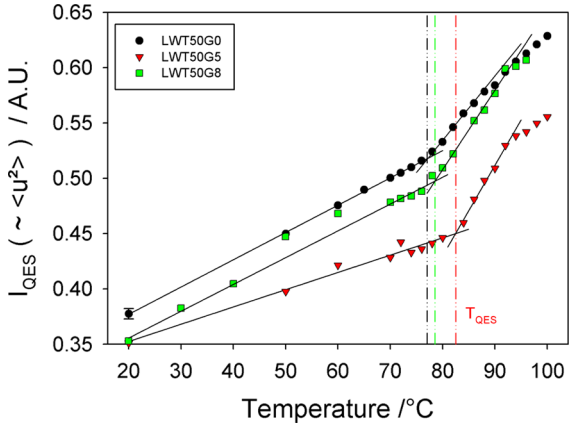

Figure 5. Quasi-elastic scattering intensity as a function of the temperature for LWT50G#. Symbols as in Figure 4. Fitting procedure to evaluate the onset temperature is drawn. A representative error bar, corresponding to ±1 SD from fitting, is shown.

interpretation as a relaxational contribution,[44] its increase with the temperature reflects a softening of the protein−solvent dynamics. In the whole investigated temperature range I_{QES} values for LWT50G0 are always higher than the ones obtained in the presence of glycerol: this agrees with the fact that glycerol reduces the fluctuations of the system. For every glycerol concentration, the peak intensity increases by increasing the temperature until it reaches a value T_{QES} in which the former linear trend is interrupted and a change in the slope occurs. Values for T_{QES} have been determined by crossing two linear fits corresponding respectively to data points before and after the slope's break. We estimated the associated uncertainties by computing the linear fit for every data set by adding/removing suitably the first and last points.

This transition looks like the protein dynamical transition observed by neutron scattering around 220 K.[49] Besides, it agrees with previous Fourier-transform-infrared and nuclear magnetic resonance observations on low-hydrated proteins where two dynamical transitions were reported around 220 and 346 K.[50] The present Raman investigations give the opportunity to analyze the latter dynamical transition in relation to structural changes in the lysozyme. This feature reveals the development of anharmonic motions of the protein−solvent system, driving the protein denaturation. Furthermore, the slope change occurs at a higher temperature in the presence of glycerol. As illustrated in Figure 5, by taking T_{QES} as representative of the activation of further motions related to the protein unfolding, we observe LWT50G5 exhibits the higher value. In agreement with what observed for the Amide I band, this supports the fact that the 5% glyc/TRE

dx.doi.org/10.1021/jp500673b | J. Phys. Chem. B XXXX, XXX, XXX−XXX

sample promotes a better stabilization of the protein with respect to 0% and 8%.

As we can observe in Figure 3, a shift toward lower frequencies for the main peak, as well as a decrease of the band around 170 cm^{-1}, characterizes the thermal evolution of $\chi''(\nu)$ for our systems. In this regard, Figure 6a shows the temperature

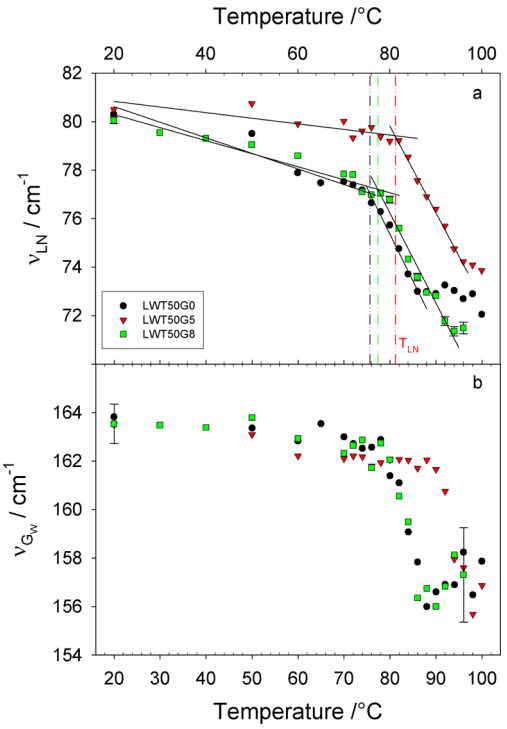

Figure 6. Panel a: temperature evolution of the vibrational frequency for LWT50G#. Fitting procedure to evaluate the onset temperature is drawn. Panel b: temperature evolution of the intermolecular O−H stretching band in the H-bond network of water for LWT50G#. Representative error bars, corresponding to ±1 SD from fitting, are shown. Symbols as in Figure 4.

dependence of the log-normal vibration peak position (ν_{LN}) for the three samples: here, the frequency's decrease by increasing the temperature reflects the same behavior observed for the I_{QES}, since a softening of the system leads toward lower frequencies of ν_{LN}. Again, an evaluation of the temperature T_{LN}, corresponding to the linear slope's break, evidences a higher value for LWT50G5. T_{LN} were determined with the same procedure used for T_{QES}. Besides, Figure 6b shows the frequency for the Gaussian peak related to water (G_W) as a function of the temperature. Since no remarkable difference is observed for the higher frequency peak G_T, related to trehalose, it can then be considered constant (data not shown). On the other hand, the G_W evolves with temperature as the log-normal vibrational peak does, showing a downshift which begins at higher temperature for LWT50G5, but no difference is evidenced among each sample at temperatures below 80 °C. We interpret our results as a weak influence of both temperature and glycerol on trehalose; instead the H-bond water network reflects what is happening to the protein. This could mean that glycerol interacts preferentially with water instead of trehalose, perturbing the H-bond network of the former. This effect is also responsible for limiting the temperature dependence of I_{QES} in Figure 5: data points in the presence of glycerol are always and systematically below the ones without glycerol, until full denaturation is achieved. In particular, 5% glyc/TRE, with respect to 0% and 8%, has a capability to stabilize the H-bond network of the solvent, limiting the softening of both the solvent and protein dynamics via their coupling. Hence the protein stability, due first of all to trehalose, is enhanced by a specific amount of glycerol (5% glyc/TRE g/g).

Protein Stability−Fast Relaxation Fluctuations Correlation. Figure 7 shows the glycerol concentration dependence

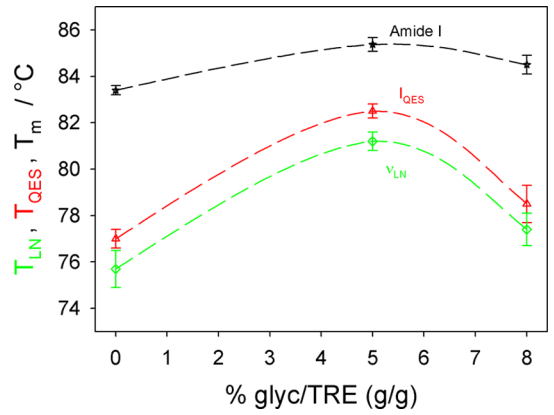

Figure 7. Amide I unfolding temperature from eq 3 (black stars); onset temperature of the QES intensity (red triangles up) and of the log-normal vibrational peak (green diamonds) as a function of the glyc/TRE weight ratio for LWT50G#. The dashed lines are a guide for eyes. Error bars are uncertainties provided by the fits.

of the unfolding temperature T_m from the Amide I analysis, along with T_{QES} and T_{LN}. Each set of data shows the same bell-like trend, drawing a maximum around 5% glyc/TRE g/g. Nevertheless, both T_{QES} and T_{LN} are lower than T_m from the Amide I band analysis. From previous investigations on protein[30] and protein−sugar[33] aqueous solutions, the vibrational component of the LFRS was found showing a softening of solvent dynamics before the unfolding was observed. That has been considered a precursor of protein denaturation. We can then explain the changes of slope in the I_{QES} and ν_{LN} as a former indication of the protein unfolding, since they are concerned with motions at the protein surface instead of those related to the protein backbone. In this regard, previous Raman scattering investigations in D_2O[33,51] and in conjunctions with temperature-modulated differential scanning calorimetry experiments[30] have revealed a precursor effect of the protein unfolding. The specific heat (c_p) jump corresponding to the denaturation was detected prior to the unfolding of secondary structure. It is usually assigned to the release of degrees of freedom. Using D_2O as solvent demonstrated that the increase of local mobility is related to the solvent penetration within the tertiary structure.[51] Such an increase upon heating can induce the exposure to the solvent of residues which were previously buried in the native globular state. This has led to describing the thermal denaturation process for LSZ as a two-stage process, in which the penetration of the solvent within the protein was observed before the unfolding. A linear correlation was also found between the matrix glass transition temperature and the denaturation temperature of the proteins embedded within.[12] This evidences a coupling between the matrix and the embedded protein dynamics. On the other hand, the β-relaxation, i.e., local mobility, was indicated to govern the protein stability in sugar−glass matrices.[18] The Raman

dx.doi.org/10.1021/jp500673b | J. Phys. Chem. B XXXX, XXX, XXX−XXX

investigations simultaneously carried out in the LFRS and the Amide I region indicate that the dynamical transition is observed prior to the unfolding of the secondary structure. This dynamical transition is in all likelihood induced by the softening of the solvent dynamics coupled to the protein one. This agrees with the previous interpretation of lysozyme denaturation as a two-state process from a complementary Raman and calorimetric analysis[30] in which the c_p jump associated with the denaturation probably corresponds to the dynamical transition observed here in the LFRS.

Moreover, if we get an insight of Figure 7, we can see how the difference between T_{QES} and T_{LN} is kept constant: this correlation represents a strong affinity between the relaxations and the vibrational motions of the systems. A correlation is also confirmed for T_m from Amide I and T_{QES}. This suggests once more a coupling between the rearrangements of the protein secondary structure and on the protein surface. The 5% glycerol content has the higher temperature values, though. This means that the glycerol has a higher stiffening effect on LWT50G5 than on the other samples. Nevertheless, one can see how the difference between Amide I T_m and T_{QES} is almost the same for LWT50G0 and LWT50G8, with respect to LWT50G5 whose temperatures are closest. A large temperature gap between T_m and T_{QES} means that the softening of the aqueous matrix and protein unfolding are more separate, whereas a smaller temperature gap indicates a tighter solvent−protein coupling. Thus, the LWT50G5 matrix is more rigid, making the protein stability improved, but, at the same time, once the matrix reaches the temperature to relax, the protein unfolding will follow immediately. This means that this peculiar glycerol content is the best to promote the protein/matrix coupling and confirms the consideration that it is more efficient than pure trehalose to preserve the protein stability, not only in dry systems but even in concentrated solutions.

CONCLUSIONS

The influence of a small amount of glycerol on the thermal stabilization of lysozyme in trehalose solutions at low water content was analyzed by Raman spectroscopy. The analysis of the Amide I band clearly reveals an enhanced thermal stabilization effect on the secondary structure for about 5% glyc/TRE content. The low-frequency investigations show a stiffening of the protein−trehalose dynamics correlated with the limitation of the fluctuation dynamics of the system, for 5% glyc/TRE content, along with stabilizing the H-bond network in the solvent. It is observed that the reduction of the amplitude of local fluctuations by trehalose is enhanced by addition of a small amount of glycerol. A correlation between protein stability and anharmonic and quasi-harmonic motions of the solvent is also evidenced, in which the latter are precursors to the larger structural and global protein unfolding. It is worth noting that only Raman spectroscopy provides detailed information on the mechanism of protein denaturation/stabilization, by measuring simultaneously the LFRS and the Amide I region. It was then indicated that the dynamical transition, i.e., the release of local motions, was a precursor of the protein unfolding. The action of the investigated bioprotectants' mixtures against high temperature is therefore related to their capability to inhibit the dynamical transition preceding the denaturation.

AUTHOR INFORMATION

Corresponding Author

*Phone: +33(0)320434708. E-mail: giuseppe.bellavia@univ-lille1.fr.

Notes

The authors declare no competing financial interest.

ACKNOWLEDGMENTS

This work was supported by ANR (Agence Nationale de la Recherche) through the BIOSTAB project ("Physique-Chimie du Vivant" program).

REFERENCES

(1) Fox, K. C. Biopreservation. Putting Proteins Under Glass. *Science* **1995**, *267*, 1922−1923.
(2) Rothschild, L. J.; Mancinelli, R. L. Life in Extreme Environments. *Nature* **2001**, *409*, 1092−1101.
(3) Roser, B. Trehalose, a New Approach to Premium Dried Foods. *Trends in Food Science & Technology* **1991**, *2*, 166−169.
(4) Carpenter, J. F.; Crowe, J. H. Is Trehalose Special for Preserving Dry Biomaterials? *Biochemistry* **1989**, *28*, 3916−3922.
(5) Belton, P. S.; Gil, A. M. IR and Raman Spectroscopic Studies of the Interaction of Trehalose with Hen Egg White Lysozyme. *Biopolymers* **1994**, *34*, 957−961.
(6) Timasheff, S. N. Protein Hydration, Thermodynamic Binding, and Preferential Hydration. *Biochemistry* **2002**, *41*, 13474−13482.
(7) Francia, F.; Dezi, M.; Mallardi, A.; Palazzo, G.; Cordone, L.; Venturoli, G. Protein-Matrix Coupling/Uncoupling in "Dry" Systems of Photosynthetic Reaction Center Embedded in Trehalose/Sucrose: The Origin of Trehalose Peculiarity. *J. Am. Chem. Soc.* **2008**, *130*, 10240−10246.
(8) Giuffrida, S.; Cottone, G.; Bellavia, G.; Cordone, L. Proteins in Amorphous Saccharide Matrices: Structural and Dynamical Insights on Bioprotection. *Eur. Phys. J. E* **2013**, *36*, 79.
(9) Heyden, M.; Bründermann, E.; Heugen, U.; Niehues, G.; Leitner, D. M.; Havenith, M. Long-Range Influence of Carbohydrates on the Solvation Dynamics of Waters. Answers from Terahertz Absorption Measurements and Molecular Modeling Simulations. *J. Am. Chem. Soc.* **2008**, *130*, 5773−5779.
(10) Ebbinghaus, S.; Kim, S. J.; Heyden, M.; Yu, X.; Heugen, U.; Gruebele, M.; Leitner, D. M.; Havenith, M. An Extended Dynamical Hydration Shell Around Proteins. *Proc. Natl. Acad. Sci. U.S.A.* **2007**, *104*, 20749−20752.
(11) Longo, A.; Giuffrida, S.; Cottone, G.; Cordone, L. Myoglobin Embedded in Saccharide Amorphous Matrices: Water-Dependent Domains Evidenced by Small Angle X-Ray Scattering. *Phys. Chem. Chem. Phys.* **2010**, *12*, 6852−6858.
(12) Bellavia, G.; Giuffrida, S.; Cottone, G.; Cupane, A.; Cordone, L. Protein Thermal Denaturation and Matrix Glass Transition in Different Protein-Trehalose-Water Systems. *J. Phys. Chem. B* **2011**, *115*, 6340−6346.
(13) Bellavia, G.; Cottone, G.; Giuffrida, S.; Cupane, A.; Cordone, L. Thermal Denaturation of Myoglobin in Water-Disaccharide Matrixes: Relation with the Glass Transition of the System. *J. Phys. Chem. B* **2009**, *113*, 11543−11549.
(14) Bellavia, G.; Cordone, L.; Cupane, A. Calorimetric Study of Myoglobin Embedded in Trehalose−Water Matrixes. *J. Therm. Anal. Cal.* **2009**, *95*, 699−702.
(15) Sampedro, J. G.; Uribe, S. Trehalose-Enzyme Interactions Result in Structure Stabilization and Activity Inhibition. The Role of Viscosity. *Mol. Cell. Biochem.* **2004**, *256*, 319−327.
(16) Cicerone, M. T.; Tellington, A.; Trost, L.; Sokolov, A. Substantially Improved Stability of Biological Agents in Dried Form the Role of Glassy Dynamics in Preservation of Biopharmaceuticals. *BioProcess Int.* **2003**, *1*, 36−47.

(17) Cicerone, M. T.; Soles, C. L. Fast Dynamics and Stabilization of Proteins: Binary Glasses of Trehalose and Glycerol. *Biophys. J.* **2004**, *86*, 3836−3845.
(18) Cicerone, M. T.; Douglas, J. F. *β*-Relaxation Governs Protein Stability in Sugar-Glass Matrices. *Soft Matter* **2012**, *8*, 2983−2991.
(19) Averett, D.; Cicerone, M. T.; Douglas, J. F.; de Pablo, J. J. Fast Relaxation and Elasticity-Related Properties of Trehalose-Glycerol Mixtures. *Soft Matter* **2012**, *8*, 4936−4945.
(20) Magazù, S.; Migliardo, F.; Affouard, F.; Descamps, M.; Telling, M. T. F. Study of the Relaxational and Vibrational Dynamics of Bioprotectant Glass-Forming Mixtures by Neutron Scattering and Molecular Dynamics Simulation. *J. Chem. Phys.* **2010**, *132*, 184512−1−184512−9.
(21) Magazù, S.; Migliardo, F.; Parker, S. F. Vibrational Properties of Bioprotectant Mixtures of Trehalose and Glycerol. *J. Phys. Chem. B* **2011**, *115*, 11004−11009.
(22) Caliskan, G.; Mechtani, D.; Roh, J. H.; Kisliuk, A.; Sokolov, A. P.; Azzam, S.; Cicerone, M. T.; Lin-Gibson, S.; Peral, I. Protein and Solvent Dynamics: How Strongly Are They Coupled? *J. Chem. Phys.* **2004**, *121*, 1978−1983.
(23) Caliskan, G.; Kisliuk, A.; Tsai, A. M.; Sokolov, A. P. Protein Dynamics in Viscous Solvents. *J. Chem. Phys.* **2003**, *118*, 4230−4236.
(24) Dirama, T. E.; Carri, G. A.; Sokolov, A. P. Coupling between Lysozyme and Glycerol Dynamics: Microscopic Insights from Molecular-Dynamics Simulations. *J. Chem. Phys.* **2005**, *122*, 114505−1−114505−8.
(25) Curtis, E.; Dirama, T. E.; Carri, G. A.; Tobias, D. J. Inertial Suppression of Protein Dynamics in a Binary Glycerol-Trehalose Glass. *J. Phys. Chem. B* **2006**, *110*, 22953−22956.
(26) Townrow, S.; Roussenova, M.; Giardiello, M. I.; Alam, A.; Ubbink, J. Specific Volume-Hole Volume Correlations in Amorphous Carbohydrates: Effect of Temperature, Molecular Weight, and Water Content. *J. Phys. Chem. B* **2010**, *114*, 1568−1578.
(27) Roussenova, M.; Murith, M.; Alam, A.; Ubbink, J. Plasticization, Antiplasticization, and Molecular Packing in Amorphous Carbohydrate-Glycerol Matrices. *J. Phys. Chem. B* **2010**, *11*, 3237−3247.
(28) Sakai, V. G.; Khodadadi, S.; Cicerone, M. T.; Curtis, J. E.; Sokolov, A. P.; Roh, J. H. Solvent Effects on Protein Fast Dynamics: Implications for Biopreservation. *Soft Matter* **2013**, *9*, 5336−5340.
(29) Simmons, D. S.; Douglas, J. F. Nature and Interrelations of Fast Dynamic Properties in a Coarse-Grained Glass-Forming Polymer Melt. *Soft Matter* **2011**, *7*, 11010−11020.
(30) Hédoux, A.; Ionov, R.; Willart, J.-F.; Lerbret, A.; Affouard, F.; Guinet, Y.; Descamps, M.; Prévost, D.; Paccou, L.; Danéde, F. Evidence of a Two-Stage Thermal Denaturation Process in Lysozyme: a Raman Scattering and Differential Scanning Calorimetry Investigation. *J. Chem. Phys.* **2006**, *124*, 014703 1−7.
(31) Hédoux, A.; Seo, J.-A.; Guinet, Y.; Paccou, L. Analysis of Cold Denaturation Mechanism of *β*-Lactoglobulin and Comparison with Thermal Denaturation from Raman Spectroscopy Investigations. *J. Raman Spectrosc.* **2011**, *43*, 16−23.
(32) Hédoux, A.; Guinet, Y.; Paccou, L. Analysis of the Mechanism of Lysozyme Pressure Denaturation from Raman Spectroscopy Investigations, and Comparison with Thermal Denaturation. *J. Phys. Chem. B* **2011**, *115*, 6740.
(33) Hédoux, A.; Willart, J.-F.; Ionov, R.; Affouard, F.; Guinet, Y.; Paccou, L.; Lerbret, A.; Descamps, M. Analysis of Sugar Bioprotective Mechanisms on the Thermal Denaturation of Lysozyme from Raman Scattering and Differential Scanning Calorimetry Investigations. *J. Phys. Chem. B* **2006**, *110*, 22886−22893.
(34) Hédoux, A.; Willart, J.-F.; Paccou, L.; Guinet, Y.; Affouard, F.; Lerbret, A.; Descamps, M. Thermostabilization Mechanism of Bovine Serum Albumin by Trehalose. *J. Phys. Chem. B* **2009**, *113*, 6119−6126.
(35) Seo, J. A.; Hédoux, A.; Guinet, Y.; Paccou, L.; Affouard, F.; Lerbret, A.; Descamps, M. Thermal Denaturation of Beta-Lactoglobulin and Stabilization Mechanism by Trehalose Analyzed from Raman Spectroscopy Investigations. *J. Phys. Chem. B* **2010**, *114*, 6675−6684.
(36) Lerbret, A.; Affouard, F.; Bordat, P.; Hédoux, A.; Guinet, Y.; Descamps, M. Low-Frequency Vibrational Properties of Lysozyme in Sugar Aqueous Solutions: A Raman Scattering and Molecular Dynamics Simulation Study. *J. Chem. Phys.* **2009**, *131*, 245103 1−10.
(37) Hédoux, A.; Guinet, Y.; Paccou, L.; Derollez, P.; Danéde, F. Vibrational and Structural Properties of Amorphous N-Butanol: a Complementary Raman Spectroscopy and X-Ray Diffraction Study. *J. Chem. Phys.* **2013**, *138*, 214506 1−8.
(38) Williams, R. W.; Dunker, A. K. Determination of the Secondary Structure of Proteins from the Amide I Band of the Laser Raman Spectrum. *J. Mol. Biol.* **1981**, *152* (4), 783−813.
(39) Surewicz, W. K.; Mantsch, H. H.; Chapman, D. Determination of Protein Secondary Structure by Fourier Transform Infrared Spectroscopy: a Critical Assessment. *Biochemistry* **1993**, *32*, 389.
(40) Ionov, R.; Hédoux, A.; Guinet, Y.; Bordat, P.; Lerbret, A.; Affouard, F.; Prevost, D.; Descamps, M. Sugar Bioprotective Effects on Thermal Denaturation of Lysozyme: Insights from Raman Scattering Experiments and Molecular Dynamics Simulation. *J. Non-Cryst. Solids* **2006**, *352*, 4430−4436.
(41) Hédoux, A.; Guinet, Y.; Descamps, M. The Contribution of Raman Spectroscopy to the Analysis of Phase Transformations in Pharmaceutical Compounds. *Int. J. Pharm.* **2011**, *417*, 17−31.
(42) Perticaroli, S.; Nickels, J. D.; Ehlers, G.; O'Neill, H.; Zhang, Q.; Sokolov, A. P. Secondary Structure and Rigidity in Model Proteins. *Soft Matter* **2013**, *9*, 9548−9556.
(43) Walrafen, G. E.; Fisher, M. R.; Hokmabadi, M. S.; Yang, W.-H. Temperature Dependence of the Low- and HigFrequency Raman Scattering from Liquid Water. *J. Chem. Phys.* **1986**, *85*, 6970−6982.
(44) Ribeiro, M. C. C. Low-Frequency Raman Spectra and Fragility of Imidazolium Ionic Liquids. *J. Chem. Phys.* **2010**, *133*, 024503 1−6.
(45) Sokolov, A. P.; Kisliuk, A.; Quitmann, D.; Duval, E. Evaluation of Density of Vibrational States of Glasses from Low-Frequency Raman Spectra. *Phys. Rev. B* **1993**, *48*, 7692−7695.
(46) Hédoux, A.; Derollez, P.; Guinet, Y.; Dianoux, A. J.; Descamps, M. Low-Frequency Vibrational Excitations in the Amorphous and Crystalline States of Triphenyl Phosphite: a Neutron and Raman Scattering Investigation. *Phys. Rev. B* **2001**, *63*, 144202.
(47) Achibat, T.; Boukenter, A.; Duval, E.; Lorentz, G.; Etienne, S. Low-Frequency Raman Scattering and Structure of Amorphous Polymers: Stretching Effect. *J. Chem. Phys.* **1991**, *95*, 2949−2954.
(48) Padrò, J. A.; Martì, J. An Interpretation of the Low-Frequency Spectrum of Liquid Water. *J. Chem. Phys.* **2003**, *118*, 452−453.
(49) Schirò, G.; Natali, F.; Cupane, A. Physical Origin of Anharmonic Dynamics in Proteins: New Insights from Resolution-Dependent Neutron Scattering on Homomeric Polypeptides. *Phys. Rev. Lett.* **2012**, *109*, 128102 (12).
(50) Mallamace, F.; Chen, S.-H.; Broccio, M.; Corsaro, C.; Crupi, V.; Majolino, D.; Venuti, V.; Baglioni, P.; Fratini, E.; Vannucci, C.; Stanley, H. E. Role of the Solvent in the Dynamical Transitions of Proteins: the Case of the Lysozyme-Water System. *J. Chem. Phys.* **2007**, *127*, 045104 (6).
(51) Bellavia, G.; Paccou, L.; Achir, S.; Guinet, Y.; Siepmann, J.; Hédoux, A. Analysis of Bulk and Hydration Water During Thermal Lysozyme Denaturation Using Raman Scattering. *Food Biophysics* **2013**, *8*, 170−176.